METALLURGY OF NON-FERROUS METALS / МЕТАЛЛУРГИЯ ЦВЕТНЫХ МЕТАЛЛОВ

UDC 662.7.662.242
https://doi.org/10.17073/0021-3438-2025-1-14-26

Research article
Научная статья

Investigation of gold dissolution in cyanide solutions using cyclic voltammetry methods

A.N. Baranov[1], **V.V. Elshin**[1], **A.A. Kolodin**[1], **E.V. Filippova**[2]

[1] **Irkutsk National Research Technical University**
83 Lermontov Str., Irkutsk 664074, Russia

[2] **Federal Service for Environmental, Industrial and Nuclear Supervision**
1 Bld, 34 Taganskaya Str., Moscow 125993, Russia

✉ Anatoly N. Baranov (baranov@istu.edu)

Abstract: The study presents the results of gold dissolution in cyanide solutions using the cyclic voltammetry method. A methodology was developed to investigate the mechanism of gold leaching in cyanide solutions by determining the relationship between current and potential under varying cyanide and oxygen concentrations. It is known that as the electrode potential increases, the gold dissolution current rises until the passivation potential is reached, after which it sharply decreases due to the formation of an oxide film, resulting in gold passivation. It was established that the maximum passivation current is achieved at oxygen and sodium cyanide concentrations of 7.5 mg/dm^3 and 300–400 mg/dm^3, respectively. Mathematical relationships for the passivation potential and current as functions of sodium cyanide and oxygen concentrations were determined, described by polynomial equations with approximation coefficients $R_2 > 0.7$. When the polarization direction is reversed, the current polarity changes, producing a cathodic curve with a peak at the depassivation potential, corresponding to the dissolution of the passive gold film. The depassivation potential and current show weak dependence on sodium cyanide concentration. The cyclic voltammetric curve terminates at the initial point with the same current and potential values, indicating the complete removal of the oxide film from the gold surface. The oxide film thickness, calculated based on the amount of passed charge, was found to be 0.007 μm. Metallographic studies demonstrated that the film thickness could not be determined by this method. A gold surface diffractogram revealed that the passive film formed after heating to 125 °C has the crystallochemical formula $Na_{0.66}Au_{2.66}O_4$. The study highlights the potential for enhancing gold recovery from refractory ores through electrochemical treatment in alkaline conditions.

Keywords: gold, cyanidation, oxygen, electrochemistry, potentiostat, passivation, depassivation, current, potential, electron microscope, cyclic voltammetry, XRD patterns, redox potential.

For citation: Baranov A.N., Elshin V.V., Kolodin A.A., Filippova E.V. Investigation of gold dissolution in cyanide solutions using cyclic voltammetry methods. *Izvestiya. Non-Ferrous Metallurgy.* 2025;31(1):14–26. https://doi.org/10.17073/0021-3438-2025-1-14-26

Исследование растворения золота в цианистых растворах методами циклической вольтамперометрии

А.Н. Баранов[1], **В.В. Ёлшин**[1], **А.А. Колодин**[1], **Е.В. Филиппова**[2]

[1] **Иркутский национальный исследовательский технический университет**
Россия, 664074, г. Иркутск, ул. Лермонтова, 83

[2] **Федеральная служба по экологическому, технологическому и атомному надзору**
Россия, 125993, г. Москва, ул. Таганская, 34, стр. 1

✉ Анатолий Никитич Баранов (baranov@istu.edu)

Аннотация: Представлены результаты исследования растворения золота в цианистых растворах с применением метода циклической вольтамперометрии. Разработана методика исследования механизма выщелачивания золота в цианистых растворах путем

определения зависимости силы тока от потенциала при различных концентрациях цианида натрия и кислорода. Известно, что с повышением электродного потенциала ток растворения золота возрастает до потенциала пассивации, а затем резко снижается в связи с образованием оксидной пленки, и происходит пассивация золота. Установлено, что максимальное значение тока пассивации достигается при концентрациях кислорода и цианида натрия в растворе 7,5 и 300–400 мг/дм^3 соответственно. Определены математические зависимости потенциала и тока пассивации от концентраций цианида натрия и кислорода, которые описываются полиномиальными уравнениями с коэффициентами аппроксимации $R^2 > 0{,}7$. При смене направления поляризации полярность тока меняется, и образуется катодная кривая с максимумом при потенциале депассивации, которая связана с растворением пассивной пленки золота. Потенциал и ток депассивации слабо зависят от концентрации цианида натрия. Циклическая вольт-амперная кривая заканчивается в начальной точке при том же значении тока и потенциала, что свидетельствует об удалении оксидной пленки с поверхности золота. Толщина оксидной пленки установлена расчетными методами с учетом количества пропущенного электричества и составляет 0,007 мкм. Металлографические исследования показали, что толщина пленки этим методом не определяется. Дифрактограмма поверхности золота свидетельствует о том, что образующаяся пассивная пленка после нагрева до температуры 125 °С имеет кристаллохимическую формулу $Na_{0,66}Au_{2,66}O_4$. Показана возможность повышения извлечения золота из упорных руд путем электрохимической обработки щелочи.

Ключевые слова: золото, цианирование, кислород, электрохимия, потенциостат, пассивация, депассивация, ток, потенциал, электронный микроскоп, циклическая вольтамперометрия, дифрактограммы, окислительно-востановительный потенциал.

Для цитирования: Баранов А.Н., Ёлшин В.В., Колодин А.А., Филиппова Е.В. Исследование растворения золота в цианистых растворах методами циклической вольтамперометрии. *Известия вузов. Цветная металлургия.* 2025;31(1):14–26.
https://doi.org/10.17073/0021-3438-2025-1-14-26

Introduction

At present, cyanidation remains the primary method for extracting gold from ore. This process involves leaching precious metals using dilute solutions of cyanide salts in the presence of atmospheric oxygen, as shown in the reaction [1]:

$$2Au + 4NaCN + 0.5O_2 + H_2O = \\ = 2NaAu(CN)_2 + 2NaOH. \quad (1)$$

Gold dissolution follows an electrochemical mechanism, in which the ionization of metal atoms depends on the electrode potential. Electrochemical studies on the dissolution of gold in cyanide solutions at varying oxygen concentrations have been conducted in studies [2—4]. It is known that increasing the anodic potential raises the current intensity, thereby enhancing gold dissolution according to Faraday's law. Once a certain potential is reached, the current intensity sharply decreases due to gold passivation. This potential is defined as the passivation potential (E_{pas}). The passive state is attributed to the formation of a protective layer on the metal surface under specific conditions due to interactions with the environment. Corrosion studies of metals have shown that the dissolution rate increases as acid concentrations rise but then drops sharply and abruptly once a specific oxidant concentration is reached. This phenomenon has been extensively documented for iron, aluminum, chromium, and other metals in acidic solutions [5]. This behavior has also been observed for gold using potentiostatic polarization measurements [6]. Cyclic voltammetry (CV) is currently employed for more detailed investigations into corrosion mechanisms [7—11]. CV methods have been used to study the electrochemical behavior of electrodes made from various materials, such as glassy carbon and graphene/glassy carbon with deposited Au nanoparticles [12]. However, data on gold dissolution in cyanide solutions using these methods are lacking.

Enhancing the efficiency of the cyanidation process is of great importance, and various methods have been employed, including hydroacoustic [12], autoclave [13—15], electrochemical [16], photochemical [14], and other treatments to influence gold dissolution processes [17—22]. These methods, to varying degrees, alter the electrode potential of the noble metal. Therefore, studying the mechanism of gold electrochemical dissolution under different conditions using CV is highly relevant. The aim of this work is to investigate the kinetics of gold dissolution in cyanide solutions through CV measurements to elucidate the dissolution mechanism and the formation of passive films on the gold surface at different oxygen and sodium cyanide concentrations.

Methodology of experiments

Electrochemical studies were conducted by recording CV dependencies in cyanide solutions using a PI-50-PRO potentiostat-galvanostat. A 0.5 dm^3 cell was

used, containing a working gold electrode with a surface area of 0.567 cm^2, a platinum auxiliary electrode (EPV-1), a silver chloride reference electrode (EVP-08), and a WTW FDO 925 dissolved oxygen sensor. The oxygen concentration in the cell was regulated by supplying either argon or compressed air.

For the experiments, solutions with sodium cyanide (NaCN) concentrations ranging from 20 to 500 mg/dm^3 and a pH of 10—10.5 were prepared. The gold electrode was immersed to its maximum possible depth near a rotating magnetic stirrer. To reduce the diffusion resistance of gold dissolution, the stirrer was set to a high speed of 650 rpm, with a potential sweep rate of 3.74 mV/s. A 0.450 dm^3 solution with a specific NaCN concentration was added to the cell. The initial oxygen concentration in the solution was 7.5 mg/dm^3. Argon was used to adjust the oxygen concentration as needed.

The PI-50-PRO potentiostat was set to a polarization range of 100 to 1000 mV in both forward and reverse directions, with a sweep rate of 3.74 mV/s. After recording CV curves, argon was introduced into the solution to reduce the oxygen concentration to a specified level, and CV measurements were repeated. Thus, the oxygen concentration was gradually reduced from 7.5 to 0.01 mg/dm^3. At the end of each experiment, the solution was drained, and the cell was rinsed. Before and after each experiment, the NaCN concentration was measured using titration. Consequently, CV curves were obtained for all prepared solutions with varying NaCN concentrations and oxygen levels.

Results and discussion

Fig. 1 shows the CV curves with potentials referenced to the silver/silver chloride (Ag/AgCl) reference electrode.

The analysis of the typical CV dependencies in Fig. 1 made it possible to determine the passivation potentials (E_{pas}) corresponding to the maximum anodic current (I_{pas}). During the reverse sweep of the CV curves, from 1000 mV to 100 mV, the current polarity changes, and at the maximum cathodic depassivation current (I_{dep}), the depassivation potential (E_{dep}) can be identified.

It is known [5] that the current density serves as an electrochemical indicator of the mass rate of electrochemical corrosion (K_m), which can be applied to the gold leaching process, as this also proceeds spontaneously in cyanide solutions:

$$K_m = qIt/S. \quad (2)$$

Here, $K_m = m/(St)$ is the corrosion rate, g/(cm^2·s);

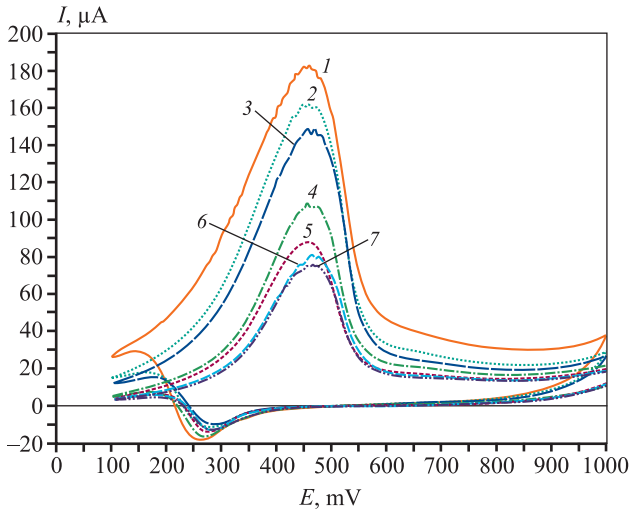

Fig. 1. Example of typical cyclic voltammograms at NaCN concentration of 200 mg/dm^3
C_{O_2}, mg/dm^3: ***1*** – 7.5; ***2*** – 3.0; ***3*** – 2.0; ***4*** – 1.3; ***5*** – 0.8; ***6*** – 0.4; ***7*** – 0.05

Рис. 1. Пример типичных цикличных вольт-амперных зависимостей при концентрации C_{NaCN} = 200 мг/$дм^3$
C_{O_2}, мг/$дм^3$: ***1*** – 7,5; ***2*** – 3,0; ***3*** – 2,0; ***4*** – 1,3; ***5*** – 0,8; ***6*** – 0,4; ***7*** – 0,05

m is the mass of dissolved gold, g; S = 0.567 cm^2 is the electrode area; *t* is time, s; $i = I/S$ is the current density, A/cm^2; *q* is the electrochemical equivalent of gold, equal to the atomic mass of gold (*A*) divided by the number of electrons (*n*) and Faraday's constant (*F*): $q = A/(nF) = 196.967/(1 \cdot 96500) = 0.00204$ g/(A·s).

At the initial stage of the CV measurements (Fig. 1), the gold corrosion rate was $I/S = 29/0.567 =$ $= 51$ μA/cm^2, while at the passivation potential, it reached $K_m = 180/0.567 = 317.5$ μA/cm^2. This indicates that the gold dissolution rate can increase by a factor of 6.2 with a 350 mV positive shift in the gold electrode potential. Further increasing the potential to 600 mV results in reduced gold dissolution due to the formation of a passive film.

Two main theories describe the nature of the passivating layer: the phase and adsorption theories of passivity. According to the phase theory, passivity arises from the formation of a relatively thick phase film on the metal surface, consisting of corrosion products that isolate the metal from the corrosive medium. The phase theory links the determining influence of potential on the transition of the metal into a passive state with changes in the composition and crystalline structure of the corrosion products, and therefore, the protective properties of the films formed as the electrode potential increases. However, an independent phase film is not

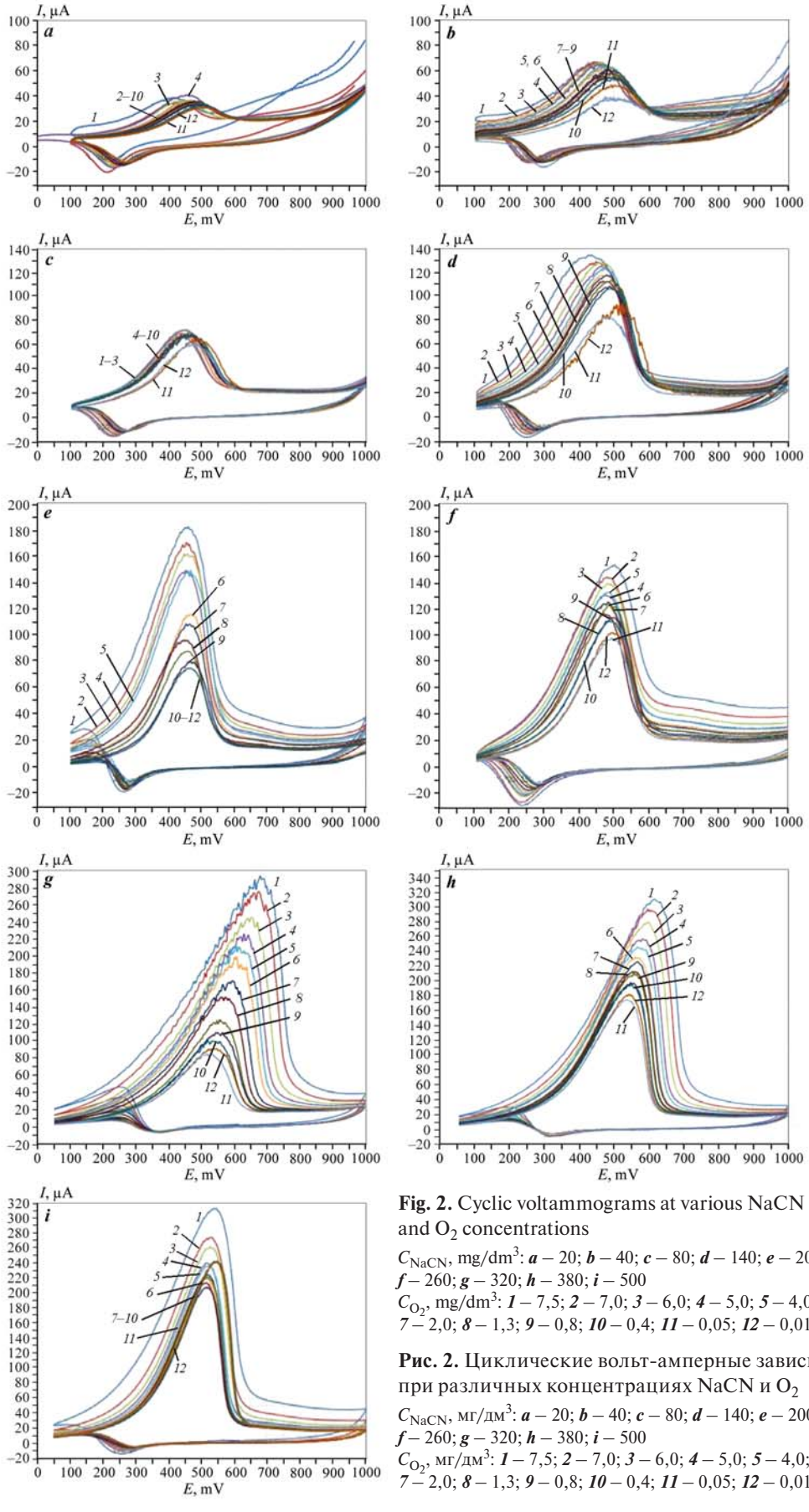

Fig. 2. Cyclic voltammograms at various NaCN and O_2 concentrations

C_{NaCN}, mg/dm^3: ***a*** – 20; ***b*** – 40; ***c*** – 80; ***d*** – 140; ***e*** – 200; ***f*** – 260; ***g*** – 320; ***h*** – 380; ***i*** – 500
C_{O_2}, mg/dm^3: ***1*** – 7,5; ***2*** – 7,0; ***3*** – 6,0; ***4*** – 5,0; ***5*** – 4,0; ***6*** – 3,0; ***7*** – 2,0; ***8*** – 1,3; ***9*** – 0,8; ***10*** – 0,4; ***11*** – 0,05; ***12*** – 0,01

Рис. 2. Циклические вольт-амперные зависимости при различных концентрациях NaCN и O_2

C_{NaCN}, мг/дм^3: ***a*** – 20; ***b*** – 40; ***c*** – 80; ***d*** – 140; ***e*** – 200; ***f*** – 260; ***g*** – 320; ***h*** – 380; ***i*** – 500
C_{O_2}, мг/дм^3: ***1*** – 7,5; ***2*** – 7,0; ***3*** – 6,0; ***4*** – 5,0; ***5*** – 4,0; ***6*** – 3,0; ***7*** – 2,0; ***8*** – 1,3; ***9*** – 0,8; ***10*** – 0,4; ***11*** – 0,05; ***12*** – 0,01

always observed on the surface of a metal in a passive state. The adsorption theory postulates that the metal transitions to a passive state due to the formation of a chemisorbed layer of an oxidant, such as oxygen, on its surface. We believe that both theories are applicable to the gold dissolution process and must be considered during gold leaching.

To establish the mechanism of gold passivation, Fig. 2 presents the CV measurement results in NaCN solutions with various oxygen concentrations (potentials are indicated in mV relative to the Ag/AgCl reference electrode).

According to the analysis of the CV dependencies (see Fig. 2), a current peak corresponding to the passivation potential is observed at various sodium cyanide concentrations. As the potential decreases from 1000 to 100 mV, the current reverses polarity, indicating the dissolution of the passive film. The maximum cathodic current, referred to as the depassivation current (I_{dep}), is reached at the depassivation potential (E_{dep}). Based on the obtained results (Fig. 2), the relationships between the passivation and depassivation currents and potentials with sodium cyanide concentration at an oxygen concentration of 7.5 mg/dm^3 were determined, as shown in Fig. 3. These relationships (Fig. 3) are described by polynomial equations of the following form:

$$E_{pas} = 360.93 + 1.0621C_{NaCN} - 0.0011C^2_{NaCN}, \quad R^2 = 0.6587, \tag{3}$$

$$I_{pas} = 12.637 + 0.9925C_{NaCN} - 0.0012C^2_{NaCN}, \quad R_2 = 0.7342, \tag{4}$$

$$E_{dep} = 229.9 + 0.3791C_{NaCN} + 0.00060012C^2_{NaCN}, \quad R_2 = 0.1954, \tag{5}$$

$$I_{dep} = 13.069 + 0.0723C_{NaCN} + 0.3797C^2_{NaCN}, \quad R^2 = 0.3797. \tag{6}$$

The analysis of the dependencies shown in Fig. 3, *a*, *b* indicates that they can be described by polynomial equations with approximation coefficients around 0.7, making them statistically significant. In contrast, the depassivation processes (Fig. 3, *c*, *d*) have lower approximation coefficients ($R_2 < 0.4$) and are not statistically significant. This suggests that the dissolution of the passive film is independent of the sodium cyanide concentration.

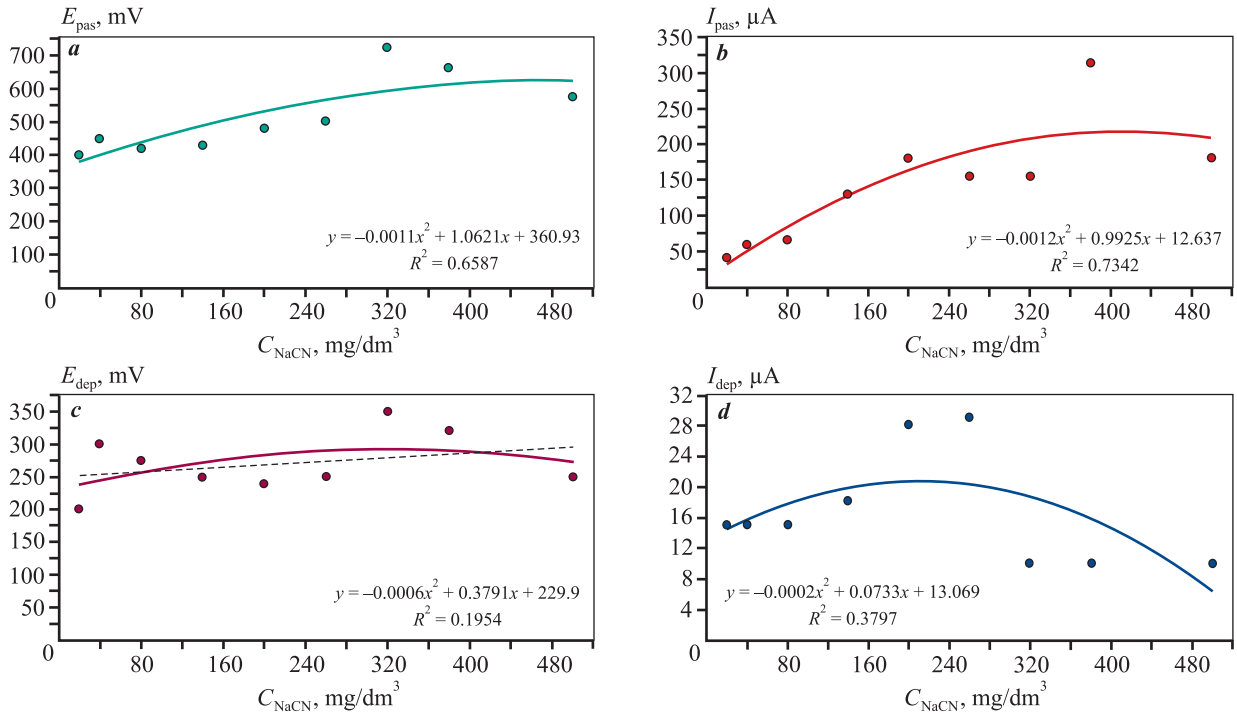

Fig. 3. Dependence of passivation potential (***a***), passivation current (***b***), depassivation potential (***c***), and depassivation current (***d***) on sodium cyanide concentration

Рис. 3. Зависимость потенциала пассивации (***a***), тока пассивации (***b***), потенциала депассивации (***c***), тока депассивации (***d***) от концентрации цианида натрия

The maximum passivation currents, according to equation (4), are reached at C_{NaCN} = 400 mg/dm^3. However, two visual maxima are observed at cyanide concentrations of 200 and 400 mg/dm^3. This could be attributed to the high uncertainty in determining the passivation current, and the application of statistical methods for data processing is necessary to improve reliability.

During the experiments, the sodium cyanide concentration in the solution was monitored before and after recording a series of CV curves at various cyanide concentrations. Fig. 4 presents the results of the reduction in NaCN concentration as a percentage of its initial value during CV measurements, with oxygen levels varying from 7.5 to 0.01 mg/dm^3 as shown in Fig. 2.

The change in sodium cyanide concentration as a function of its initial concentration is described by the following polynomial equation:

$$C_{NaCN} = 0.2776C_{н\,NaCN} - 0.0004C^2_{н\,NaCN} - 28.584, \quad R_2 = 0.9649. \tag{7}$$

The maximum reduction in NaCN concentration is 25.3 % at an initial sodium cyanide concentration of 370 mg/dm^3. Given that 0.45 dm^3 of solution was added to the cell, the maximum NaCN loss amounts to 42 mg during 12 CV measurements at different oxygen concentrations in a sodium cyanide solution with an initial concentration of 370 mg/dm^3.

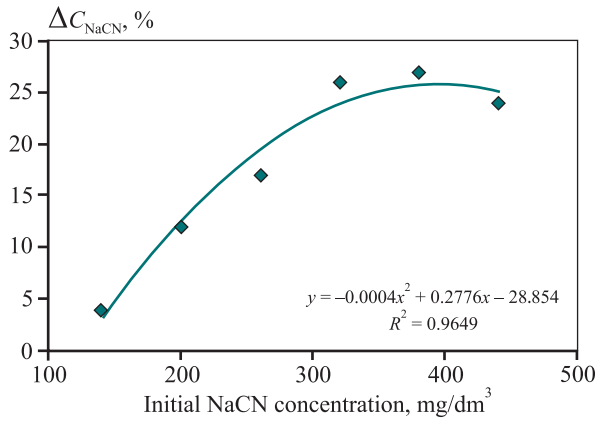

Fig. 4. Reduction in sodium cyanide concentration based on its initial concentration during CV measurements with varying oxygen levels

Рис. 4. Снижение концентрации цианистого натрия в зависимости от начальной его концентрации при снятии серии ЦВА с различной концентрацией кислорода

To provide more comprehensive information for selecting optimal leaching conditions based on oxygen concentration, three-dimensional diagrams were constructed to show the dependence of current or potential on sodium cyanide and oxygen concentrations.

Figures 5 and 6 present three-dimensional diagrams illustrating the dependence of current and potential on sodium cyanide and oxygen concentrations.

According to Fig. 5, the maximum passivation potential reaches 600 mV at a cyanide concentra-

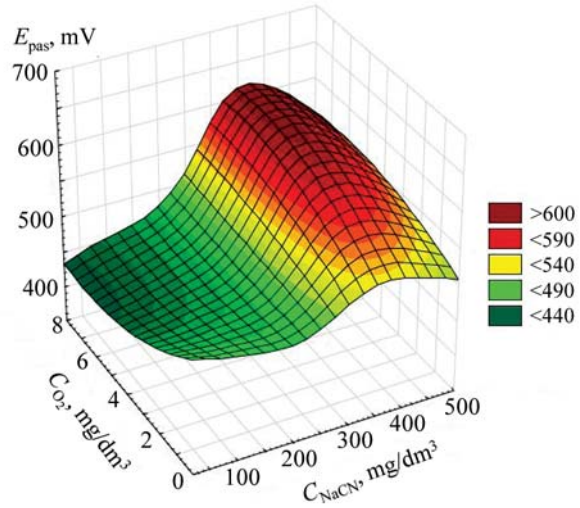

Fig. 5. Dependence of passivation potential on NaCN and O_2 concentration

Рис. 5. Диаграмма зависимости потенциала пассивации от концентраций NaCN и O_2

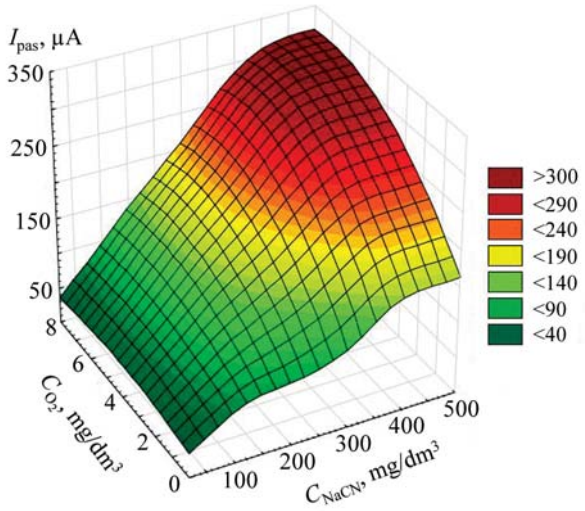

Fig. 6. Dependence of passivation current on NaCN and O_2 concentration

Рис. 6. Диаграмма зависимости тока пассивации от концентраций NaCN и O_2

tion of 400 mg/dm^3 and an oxygen concentration of 7.5 mg/dm^3.

According to Fig. 6, the maximum passivation current of 300 μA is observed at C_{NaCN} = 380 mg/dm^3 and C_{O_2} = 7.5 mg/dm^3. Notably, at an oxygen concentration of 0.05 mg/dm^3, the passivation current, and consequently the gold solubility, is 50 μA. This indicates that gold dissolves in cyanide solutions under anodic polarization even in the absence of oxygen. If oxygen does not participate in gold dissolution via reaction (1), the mechanism of anodic gold dissolution can be represented by the following reactions:

$$Au + 2(CN)^- - 2e = Au(CN)_2^-. \quad (8)$$

At the cathode, in the presence of oxygen, electrons are consumed by oxygen:

$$O_2 + 2H_2O + 2e = 4OH^-. \quad (9)$$

In the absence of oxygen, electrons are consumed during hydrogen evolution at the auxiliary platinum electrode:

$$2H^+ + 2e = H_2. \quad (10)$$

In [1], it was demonstrated that cyanide gold can form during leaching without anodic polarization via the following mechanism:

$$Au^+ + CN^- = AuCN. \quad (11)$$

This is possible considering that gold in the ore is often in contact with metal sulfides (pyrite, galena, etc.) that have high positive potentials. Cyanide gold does not dissolve directly but reacts with excess cyanide to form a complex compound, dicyanoaurate, which is capable of entering the solution:

$$AuCN + NaCN = Na[Au(CN)_2]. \quad (12)$$

Thus, to enhance the electrochemical dissolution of gold, it is recommended to increase the oxygen concentration and the electrode potential up to the passivation potential. When the electrode potential in a cyanide solution of 380 mg/dm^3 exceeds the passivation potential of 450 mV, a passive film forms, leading to a sharp decrease in current and, consequently, in gold dissolution.

To calculate the thickness of the passive gold film during CV measurements, the following electrochemical reaction occurring at the anode was considered: $Au - 1e = Au^+$. The obtained CV curves (see Fig. 2, *e*) show that as the potential increases, the current rises, and the amount of dissolved gold (m) can be calculated using Faraday's law:

$$m = qIt, \quad (13)$$

where I is the current, A; t is the time, s; q is the electrochemical equivalent of gold, equal to 0.002 g/(A·s).

The time can be determined based on the potential sweep rate v = 3.74 mV/s during CV measurements: $t = (E_{pas} - E_n)/v = (450 - 100)/3.74 = 93.58$ s. The current is obtained from the I—E (see Fig. 1) as the average between the initial current and the maximum current: $I = (182 - 27)/2 = 77.5$ μA = $77.5 \cdot 10^{-6}$ A. Let us calculate the amount of dissolved gold during a single CV measurement at a sodium cyanide concentration of 200 mg/dm^3 (see Fig. 1). For one CV measurement, the amount of dissolved gold is: $m = qIt = 0.002 \cdot 77.5 \cdot 10^{-6} \times \times 93.58 = 14.5 \cdot 10^{-6}$ g = 14.5 μg.

During passivation, the current decreases to its initial state, and a passive film forms through the following reactions: $Au - 3e = Au^{3+}$, $Au^{3+} + 3OH^- = = Au(OH)_3$. The amount of dissolved gold, based on equation (13), is $m = qIt = 0.00068 \cdot 77.5 \cdot 10^{-6} \cdot 93.58 = = 4.93 \cdot 10^{-6}$ g, where the electrochemical equivalent for Au^{3+} is 0.00068 g/(A·s). The mass of the passive $Au(OH)_3$ film (molecular mass = 237) can be calculated stoichiometrically as $237 \cdot 4.93 \cdot 10^{-6}/196.97 = = 5.93 \cdot 10^{-6}$ g. The thickness of the film is determined [23] by dividing the film mass by the product of the electrode area and the film density. Since the density of the film is not provided in reference data, it is calculated based on the additive properties of the specific densities. Considering that $Au(OH)_3$ contains 0.784 parts gold (ρ = 19.3 g/cm^3) and 0.215 parts $(OH)_3$ (ρ = 1 g/cm^3), the film density is 14.9 g/cm^3. The film thickness, given the electrode area of 0.567 cm^2, is calculated as $h = 5.93 \cdot 10^{-6}/(0.567 \cdot 14.9) = 0.7 \cdot 10^{-6}$ cm = = 0.007 μm. Table 1 presents the results of the calculations for the mass of dissolved gold, the stoichiometric calculation of cyanide consumption based on reaction (1) considering the mass of dissolved gold, and the calculated thickness of the passive film in the CV region, accounting for the formation of gold hydroxide.

The calculated thickness of the passive film (0.007 μm) is significantly smaller than passive films formed on metals like aluminum (0.01—1 μm). It is likely that the adsorption theory of passivity applies to films on gold, where a sharp decrease in anodic current occurs due to the formation of a chemisorbed oxygen layer, as observed on platinum with 1—6 % monolayer oxygen coverage [23]. Based on sodium cyanide consump-

Table 1. **Results of passive film thickness calculations**

Таблица 1. Результаты расчетов толщины пассивной пленки

CV range, mV (see Fig. 2, *e*)	Mass of dissolved gold, μg	Cyanide consumption per reaction (1), μg	Calculated passive film thickness, μm
100–450 (old dissolution)	4.94	2.54	–
450–700 (passive film formation)	5.96	2.97	0.007
Results of 12 CVs (at various oxygen concentrations)	130.9	66.1	–

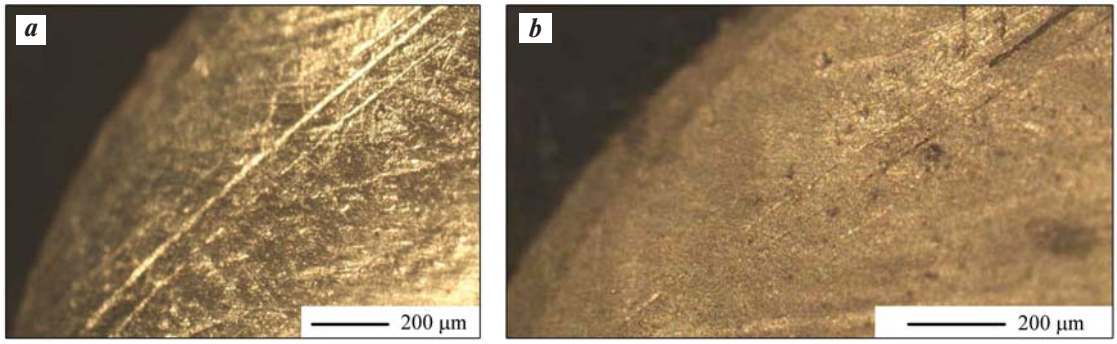

Fig. 7. Microstructures of the gold electrode before passivation (***a***) and after passivation (***b***)

Рис. 7. Микроструктуры золота на электроде до пассивации (***a***) и после пассивации (***b***)

tion, previous calculations showed that during 12 CV measurements, the reduction in cyanide concentration amounted to 42 mg, which greatly exceeds the amount required for the electrochemical dissolution of gold ($66.1 \cdot 10^{-6}$ g). This suggests that sodium cyanide decomposes during CV measurements.

To determine the actual thickness of the films on the obtained gold samples, metallographic studies were conducted. Microstructure imaging was performed using an inverted metallographic microscope (Olympus GX-51). Fig. 7 shows the microstructures of the gold electrode before and after passivation.

In Fig. 7, *a*, the clean gold surface shows visible lines from grinding and polishing. In Fig. 7, *b*, after passivation, the surface appears gray with no signs of roughness—likely due to the formation of a gold oxide film, the thickness of which cannot be determined using this method.

To investigate the composition of the film, a fragment of the Pourbaix diagram for gold is provided in Fig. 8 [24; 25].

The *E*—pH diagram for the Au—H_2O system indicates that gold hydroxide ($Au(OH)_3$) forms at pH = = 2÷11 and $E > 0.8$ V. At pH = 10 and $E > 2.0$ V AuO_2 is expected to form. Accordingly, on the recorded CV dependencies (see Fig. 2) at pH = 10 and $E > 0.8$ V, $Au(OH)_3$ likely forms. However, it is important to note that the Pourbaix diagram pertains to aqueous solutions, whereas the passive film in this study was formed in sodium cyanide solutions. To determine the composition of the passive film, an *X*-ray diffraction (XRD) analysis was performed using a Shimadzu XRD-7000 automatic powder diffractometer. A pure gold sample (1 cm^2) was prepared by grinding, polishing, degreasing in acetone, rinsing with distilled water, and passivating in a sodium cyanide solution (200 mg/dm^3) at $E > 650$ mV for 1 h. After drying at room temperature, the surface of the gold sample exhibited a dark brown coloration. The diffraction pattern of the passivated sample revealed no characteristic peaks corresponding to gold oxides or hydroxides, indicating that the passive film lacks a crystalline structure. According to [26; 27], gold hydroxide undergoes dehydration upon heating to 125 °C, initially forming AuO(OH), followed by sesquioxide (Au_2O_3), which decomposes into Au and O_2 at temperatures exceeding 160 °C. Therefore, in the second stage of the investigation, the gold sample was heated at 125 °C for 1 hour prior to recording the dif-

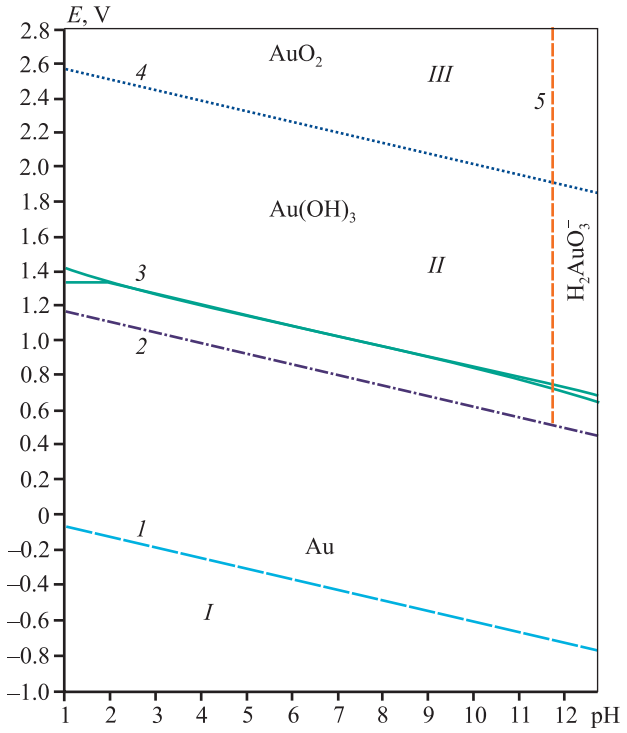

Fig. 8. Pourbet diagram for the Au–H_2O system at 25 °C [24; 25]
1, ***2*** – equilibrium lines of the hydrogen and oxygen electrodes;
3 – equilibrium line Au–$Au(OH)_3$; ***4*** – equilibrium line $Au(OH)_3$–AuO_2;
5 – equilibrium line AuO_2–$H_2AuO_3^-$
I – region of thermodynamic stability of gold; ***II*** – region of gold hydroxide ($Au(OH)_3$) formation; ***III*** – region of gold dioxide (AuO_2) formation

Рис. 8. Диаграмма Пурбе для системы Au–H_2O при температуре 25 °C [24; 25]
1, ***2*** – линии равновесия водородного и кислородного электродов;
3 – равновесная линия Au–$Au(OH)_3$; ***4*** – равновесная линия $Au(OH)_3$–AuO_2; ***5*** – равновесная линия AuO_2–$H_2AuO_3^-$
I – область термодинамической устойчивости золота;
II – область образования гидроксида золота $Au(OH)_3$;
III – область образования диоксида золота AuO_2

fraction pattern to further analyze the composition of the passive film.

Fig. 9 shows the diffraction pattern of the gold sample after passivation and heating, identifying the following compounds and their respective contents: Au (83 %); Au(CN) (0.05 %); $Na_{0.66}Au_{2.66}O_4$ (14 %); Cu (3 %). This indicates that sodium, cyanide, and oxygen participate in forming the passive film on gold. For the first time, a compound with the crystallochemical formula $Na_{0.66}Au_{2.66}O_4$, has been discovered, which can be interpreted as a double salt of the type $m(Na_2O)n(Au_2O_3)$. This compound was likely formed as a result of heating the gold sample. Consequently, the passive film in sodium cyanide solution consists of a hydroxide compound mNa(OH)nAu$(OH)_3$, which exists in an amorphous phase and does not produce diffraction lines. This supports the conclusion that gold passivation aligns with the adsorption theory of passivity.

Analyzing the obtained CV results on gold suggests the following dissolution mechanism. At an initial steady-state potential of 100 mV, the dissolution current ranges from 5 to 25 μA, depending on the oxygen concentration in the solution. During anodic polarization, the current increases exponentially, reaching 70—180 μA, with gold solubility increasing by a factor of 7—14, depending on the oxygen concentration. When the potential reaches 400—450 mV, the current increase stops. As an oxide film, mNa(OH)nAu$(OH)_3$, forms, the current decreases to 5—25 μA (depending on the oxygen concentration) at a complete passivation potential of 600 mV. This well-known property of metal passivation is generally attributed to the formation of an oxide film. Passivation is a well-documented phenomenon associated not only with electrode polarization but also with the oxidative properties of the environment. For example, iron dissolves readily in sulfuric acid solutions but hardly dissolves in concentrated sulfuric acid. This factor should also be considered for gold. In gold extraction plants, setting an electrode potential of 400 mV on gold via electrochemical methods is challenging. However, such tests were conducted in [16], where the pulp was subjected to electrochemical treatment on insoluble electrodes. Although the change in gold potential was not monitored, which prevented theoretical justification of the optimal current and potential during pulp treatment, an increase in gold recovery was observed.

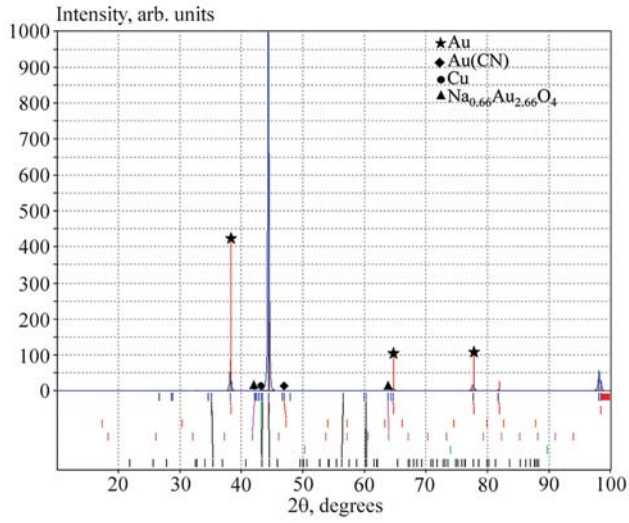

Fig. 9. XRD pattern of the gold sample after passivation and heating at 125 °C

Рис. 9. Дифрактограмма образца золота, подвергнутого пассивации и нагреву при температуре 125 °C

Table 2. **Results of gold leaching in cyanide solutions with electrochemically treated alkali**

Таблица 2. Результаты исследований выщелачивания золота в цианистых растворах с добавкой электрохимически обработанной щелочи

Alkali treatment	Amount, μg/L		Content, mg/L						
	Ag	Au	S	As	Cu	Fe	Mn	Ni	Co
Untreated	0.28	2.2	115.0	0.29	<0.001	<0.05	0.013	0.040	0.023
Electrochemically treated (10 min)	0.31	2.8	130.0	0.34	<0.001	<0.05	0.0043	0.059	0.021

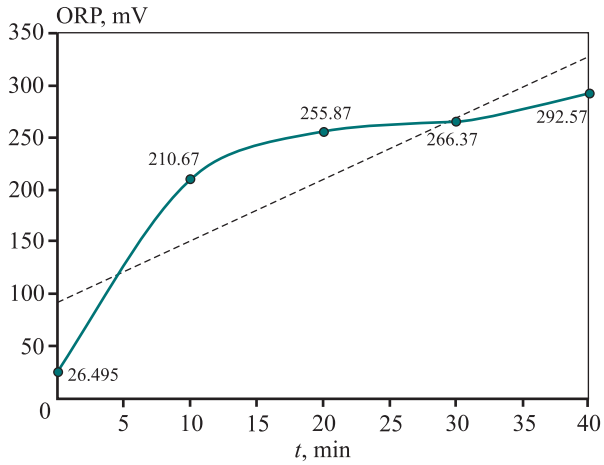

Fig. 10. Dependence of the redox potential of a 0.2 % alkali solution on treatment time on nickel electrodes at a current density of 0.1 A/cm^2

Рис. 10. Зависимость окислительно-восстановительного потенциала раствора 0,2 % щелочи от времени его обработки на никелевых электродах при плотности тока 0,1 А/см^2

Another approach to modifying the gold potential involves the use of oxidants or reductants, which shifts the resulting gold dissolution potential into the passivation and depassivation range. The redox potential (ORP) of the pulp can be increased by introducing oxidants such as oxygen, ozone, or hydrogen peroxide. Electrochemical treatment of reagents, such as an alkali solution, can also increase the ORP. Using such treated alkali in cyanide leaching enhances gold recovery. Laboratory studies on the electrochemical treatment of alkali in an electrolyzer demonstrated the potential for increasing ORP [28]. The dependence of ORP on treatment time is shown in Fig. 10.

Electrochemical treatment of alkali at optimal current and potential values for 10 minutes increases the ORP by a factor of 8.

Table 2 presents the results of gold leaching from refractory ores in cyanide solutions with the addition of electrochemically treated alkali [28].

Table 2 demonstrates that the application of electrochemically treated alkali results in an 18 % and 15 % increase in the extraction of gold and silver into the solution, respectively. Thus, to optimize the gold leaching process at extraction facilities, it is crucial to systematically monitor the electrode potential of gold and regulate it through the addition of oxidizing or reducing agents, or by employing electrochemical treatment of the pulp or reagents.

Conclusion

The cyclic voltammetric measurements on a gold electrode in cyanide solutions at varying oxygen concentrations revealed the relationship between passivation current and potential with sodium cyanide concentration. It was found that increasing the electrode potential leads to a rise in current, and upon reaching the passivation potential, a passive film forms. This results in a significant decrease in current and, consequently, a reduction in gold dissolution. The thickness of the passive film, calculated based on the charge passed during CV measurements, was determined to be 0.007 μm. *X*-ray diffraction analysis of the gold sample's surface indicated that after heating to 125°C, the passive film had the crystallochemical formula $Na_{0,66}Au_{2,66}O_4$. This film likely forms when a gold hydroxide passive film of the type nNa(OH)mAu(OH)$_3$, which is amorphous and undetectable via diffraction, is subjected to heating. The study highlights the potential for enhancing gold recovery from refractory ores through the use of electrochemically treated alkali.

References

1. Leonov S.B., Bubeev P.P., Elshin V.V. Dissolution peculiarities of gold in alkaline oxygen-bearing sodium cyanide solutions. In: *Proc. 5th Southern Hemi-Sphere Meeting Technology.* Buenos Aires, Argentina, 1997. P. 205.

2. Baranov A.N., Elshin V.V., Kolodin A.A. Electrochemical studies of gold dissolution in cyanide solutions at various oxygen concentrations. *Theory and Process Engineering of Metallurgical Production*. 2023;(1):11—17. (In Russ.).
Баранов А.Н., Елшин В.В., Колодин А.А. Электрохимические исследования растворения золота в цианистых растворах при различных концентрациях кислорода. *Теория и технология металлургического производства*. 2023;(1):11—17.
3. Elshin V.V., Kolodin A.A. Optimal control of the gold dissolution process in the gold ore grinding cycle. *Automation in Industry*. 2023;(6):8—13. (In Russ.).
https://doi.org/10.25728/avtprom.2023.06.03
Елшин В.В., Колодин А.А. Оптимальное управление процессом растворения золота в цикле измельчения золотосодержащих руд. *Автоматизация в промышленности*. 2023;(6):8—13.
https://doi.org/10.25728/avtprom.2023.06.03
4. Aleksandrov A.L., Baranov A.N. Corrosion studies of the behavior of gold in cyanide solutions. In: *Processing of natural and man-made raw materials*. Irkutsk: INRTU, 2017. P. 72–75. (In Russ.).
Александров А.Л., Баранов А.Н. Коррозионные исследования поведения золота в цианистых растворах. В сб.: *Переработка природного и техногенного сырья*. Иркутск: Изд-во ИРНИТУ, 2017. С. 72—75.
5. Bastidas D.M. Corrosion and protection of metals. *Metals*. 2020;10(4):458. https://doi.org/10.3390/met10040458
6. Azizi A., Petre C.F., Olsen C., Larachi F. Electrochemical behavior of gold cyanidation in the presence of a sulfide-rich industrial ore versus its major constitutive sulfide minerals. *Hydrometallurgy*. 2010;101:108—119.
https://doi.org/10.1016/j.hydromet.2009.12.004
7. Frankenthal R.P., Thompson D.E. The anodic behavior of gold in sulfuric acid solutions. Effect of chloride and electrode potential. *Journal of the Electrochemical Society*. 1976;123(66):799.
8. Nguyen V.Ch., Astafeva N.A., Balanovsky A.E., Baranov A.N. Study of corrosion resistance of doped surface layer with CuSn—Cr_xC_y composition after plasma hardening. *Uprochnyayushchie tekhnologii i pokrytiya*. 2021;17(5):215—220. (In Russ.).
Нгуен В.Ч., Астафьева Н.А., Балановский А.Е., Баранов А.Н. Исследование коррозионной стойкости легированного поверхностного слоя составом CuSn—Cr_xC_y после плазменного упрочнения. *Упрочняющие технологии и покрытия*. 2021;17(5):215—220.
9. Rybalka K.V., Beketaeva L.A., Davydov A.D. Estimation of AISI 1016 steel corrosion rate by polarization curves analysis and ohmic resistance measurement. *Russian Journal of Electrochemistry*. 2021;57(1):19—24. (In Russ.).
https://doi.org/10.31857/S0424857021010096
Рыбалка К.В., Бекетаева Л.А., Давыдов А.Д. Оценка скорости коррозии стали AISI 1016 анализом поляризационных кривых и методом измерения омического сопротивления. *Электрохимия*. 2021;57(1):19—24.
https://doi.org/10.31857/S0424857021010096
10. Beketaeva L.A., Rybalka K.V., Davydov A.D. Estimation of corrosion rate of cobalt-chromium alloy Starbond-CoS in NaCl solution. *Russian Journal of Electrochemistry*. 2021;57(5):309—315. (In Russ.).
https://doi.org/10.31857/S0424857021040034
Бекетаева Л.А., Рыбалка К.В., Давыдов А.Д. Оценка скорости коррозии кобальт-хромового сплава Starbond-CoS в растворе NaCl. *Электрохимия*. 2021;57(5):309—315.
https://doi.org/10.31857/S0424857021040034
11. Liu M., Lao J., Wang H., Su Z., Liu J., Wen L., Yin Z., Luo K., Peng H. Electrochemical determination of tyrosine on glassy carbon electrode modified with graphene composite and gold nanoparticles. *Russian Journal of Electrochemistry*. 2021;57(1):47—58. (In Russ.).
https://doi.org/10.31857/S0424857020110067
Лиу М., Лао Ж., Ван Х., Су З., Лиу Ж., Вен Л., Йин З., Луо К., Пен Х. Электрохимическое определение тирозина на стеклоуглеродном электроде, модифицированном композитом графена и наночастицами золота. *Электрохимия*. 2021;57(1):47—58.
https://doi.org/10.31857/S0424857020110067
12. Strizhko L.S., Bobozoda Sh.K., Novakovskaya A.O., Boboev I.R. Process control and prediction of raw material leaching using a hydroacoustic emitter. *Systems. Methods. Technologies*. 2014;(4):115—122. (In Russ.).
Стрижко Л.С., Бобозода Ш.К., Новаковская А.О., Бобоев И.Р. Управление процессом и прогнозирование выщелачивания сырья с применением гидроакустического излучателя. *Системы. Методы. Технологии*. 2014;(4):115—122.
13. Elshin V.V., Kolodin A.A., Ovsyukov A.E., Malchikhin A.S. Features of cyanide leaching of gold in the grinding cycle. *Metallurg*. 2013;(7):86—90. (In Russ.).
Елшин В.В., Колодин А.А., Овсюков А.Е. Мальчихин А.С. Особенности цианистого выщелачивания золота в цикле измельчения. *Металлург*. 2013;(7):86—90.
14. Conway M.H., Gale D.C. Sulfur's impact on the size of pressure oxidation autoclaves. *The Journal of the Minerals, Metals & Materials Society*. 1990;42:19—22.
https://doi.org/10.1007/BF03221072
15. Mason P.G. Energy requirements for the pressure oxidation of gold-bearing sulfudes. *The Journal of the Minerals, Metals & Materials Society*. 1990;42(9):15—18.
16. Lavrov A.Yu. The effectiveness rise of developing ore deposits on the basis of innovative geoecological technologies with photo-electrochemical components' activity of technological systems. *Vestnik Zabaikal's-kogo Gosudarstvennogo Universiteta*. 2013;(2):31—37. (In Russ.).

Лавров А.Ю. Повышение эффективности освоения рудных месторождений на основе использования инновационных геотехнологий с фотоэлектрохимической активацией компонентов технологических систем. *Вестник Забайкальского государственного университета*. 2013;(2):31—37.

17. Bellec S., Hodouin D., Bazin C., Khalesi M.R., Duchesne C. Modelling and simulation of gold ore leaching. In: *World Gold Conference 2009*. The Southern African Institute of Mining and Metallurgy, 2009. P. 51—59.
18. Nikoloski A.N., Nicol M.J. The electrochemistry of the leaching reactions in the Caron process. II. Cathodic processes. *Hydrometallurgy*. 2010;(105):54—59.
19. Robertson S., Jeffrey M., Zhang H., Ho E. An introductory electrochemical approach to studying hydrometallurgical reactions. *Metallurgical and Materials Transactions B*. 2005;36:313—325.
20. Shchadov I.M., Filippova E.V. Prospects for the use of new environmental protection technology in the processing of gold-bearing technogenic formations. *Ecology and Industry of Russia*. 2017;21(12):24—27. (In Russ.).
https://doi.org/10.18412/1816-0395-2017-12-24-27
Щадов И.М., Филиппова Е.В. Перспективы применения новой экологозащитной технологии при переработке золотосодержащих техногенных образований. *Экология и промышленность России*. 2017;21(12):24—27.
https://doi.org/10.18412/1816-0395-2017-12-24-27
21. Filippova E.V. New integrated technology for processing industrial wastes which allows to increase ecological safety. *Systems. Methods. Technologies*. 2016;(3):192—197. (In Russ.).
https://doi.org/10.18324/2077-5415-2016-3-192-197
Филиппова Е.В. Новая комплексная технология отработки техногенных отходов, позволяющая повысить экологическую безопасность. *Системы. Методы. Технологии*. 2016;(3):192—197.
https://doi.org/10.18324/2077-5415-2016-3-192-197
22. Syed S. Recovery of gold from secondary sources. *Hydrometallurgy*. 2012;115:31—51.
23. Baranov A.N. Corrosion and protection of metals. Irkutsk: INRTU, 2015. 178 p. (In Russ.).
Баранов А.Н. Коррозия и защита металлов: Учеб. пос. Иркутск: ИРНИТУ, 2015. 178 с.
24. Chemist's handbook. 2 nd ed. Vol. 3. Moscow: Khimya, 1964, 1025 p. (In Russ.).
Справочник химика. 2-е изд. Т. 3. М.: Химия, 1964. 1025 с.
25. Chemical encyclopedia. Vol. 2. Ed. I.A. Kiuyants. Moscow: Sovetskaya Entsiklopediya, 1990. 617 p. (In Russ.).
Химическая энциклопедия в 5 т. Т. 2. Под ред. И.А. Киуянц. М.: Советская энциклопедия, 1990. 617 с.
26. Takeno Naoto. Atlas of Eh—pH diagrams (Intercomparison of thermodynamic databases): Geological Survey of Japan Open File Report No. 419. Tsukuba, Ibaraki, Japan: National Institute of Advanced Industrial Science and Technology, Research Center for Deep Geological Environments, 2005.
27. Fenge Lin, David Vera Anaya, Shu Gong, Lim Wei Yap, Yan Lu, Zijun Yong, Wenlong Cheng. Gold nanowire sponge electrochemistry for permeable wearable sweat analysis comfortably and wirelessly. *ACS Sensors*. 2024;9(10):5414—5424.
https://doi.org/10.1021/acssensors.4c01635
28. Sidorov D.S., Baranov A.N. Intensification of leaching of non-ferrous metals using electrochemical treatment of alkali. In: *Prospects for the development of technology for processing hydrocarbon mineral resources:* Materials of the 10th All-Russ. Scientific and Practical Conf. with International Participation (Irkutsk, 22–24 April 2020). Irkutsk: INRTU, 2020. P. 51–53. (In Russ.).
Сидоров Д.С., Баранов А.Н. Интенсификация выщелачивания цветных металлов с применением электрохимической обработки щелочи. В сб.: *Перспективы развития технологии переработки углеводородных минеральных ресурсов:* Материалы X Всерос. науч.-практ. конференции с междунар. участием. Иркутск: ИРНИТУ, 2020. С. 51—53.

Information about the authors

Anatoly N. Baranov – Dr. Sci. (Eng.), Prof., Department of metallurgy of non-ferrous metals, Irkutsk National Research Technical University (INRTU).
https://orcid.org/0000-0001-5336-6522
E-mail: baranov@istu.edu

Viktor V. Elshin – Dr. Sci. (Eng.), Prof., Head of the Department of automation and control, INRTU.
https://orcid.org/0000-0002-04447-4831
E-mail: dean_zvf@.istu.edu

Alexey A. Kolodin – Senior Lecturer, Department of automation and control, INRTU.
https://orcid.org/0000-0003-4451-4014
E-mail: kolodin@istu.edu

Elena V. Filippova – Cand. Sci. (Eng.), Associate Prof., Deputy Head of the Department of assessments, licensing and inspections of nuclear fuel cycle facilities, Federal Service for Environmental, Industrial and Nuclear Supervision.
https://orcid.org/0009-0003-0872-314X
E-mail: filena78@mail.ru

Информация об авторах

Анатолий Никитич Баранов – д.т.н., профессор кафедры металлургии цветных металлов Иркутского национального исследовательского технического университета (ИРНИТУ).
https://orcid.org/0000-0001-5336-6522
E-mail: baranov@istu.edu

Виктор Владимирович Ёлшин – д.т.н., профессор, заведующий кафедрой автоматизации и управления ИРНИТУ.
https://orcid.org/0000-0002-04447-4831
E-mail: dean_zvf@.istu.edu

Алексей Александрович Колодин – ст. преподаватель кафедры автоматизации и управления ИРНИТУ.
https://orcid.org/0000-0003-4451-4014
E-mail: kolodin@istu.edu

Елена Владимировна Филиппова – к.т.н., доцент, зам. начальника отдела оценок, лицензирования и инспекций объектов ядерного топливного цикла Федеральной службы по экологическому, технологическому и атомному надзору.
https://orcid.org/0009-0003-0872-314X
E-mail: filena78@mail.ru

Contribution of the authors

A.N. Baranov – development of the main concept, formulation of the study's goal and objectives, preparation of the manuscript, and formulation of conclusions.

V.V. Elshin – scientific supervision, provision of resources, text revision, and refinement of conclusions.

A.A. Kolodin – calculations, sample testing, and manuscript preparation.

E.V. Filippova – experiment preparation, conducting experiments, manuscript drafting, and conclusion formulation.

Вклад авторов

А.Н. Баранов – формирование основной концепции, постановка цели и задачи исследования, подготовка текста статьи, формулировка выводов.

В.В. Ёлшин – научное руководство, обеспечение ресурсами, корректировка текста статьи, корректировка выводов.

А.А. Колодин – осуществление расчетов, проведение испытаний образцов, подготовка текста статьи.

Е.В. Филиппова – подготовка экспериментов и их проведение, подготовка текста статьи, формулировка выводов.

The article was submitted 20.02.2024, revised 06.09.2024, accepted for publication 19.09.2024

Статья поступила в редакцию 20.02.2024, доработана 06.09.2024, подписана в печать 19.09.2024